Database of Inlet and Exhaust Noise Shielding for Wedge-Shaped Airframe

Carl H. Gerhold and Lorenzo R. Clark
Langley Research Center, Hampton, Virginia

April 2001

Acknowledgments

Available from:

Summary

An experiment to quantify the shielding of inlet-radiated noise was performed on a scale model of an advanced, unconventional, subsonic transport concept, the blended wing body. The experiment verified significant inlet noise shielding, but the model could not be altered; therefore the effects of the variation of design parameters could not be assessed. A follow-on experiment was developed by using a simplified wedge-shaped airframe, for which the engine nacelle placement is varied. The noise shielding database from this follow-on experiment will be used to validate an insertion loss analytical code that is underway by researchers at the Langley Research Center. The experimental study was conducted in the Langley Anechoic Noise Research Facility. A high frequency, wideband, omnidirective sound source was placed in a simulated engine nacelle at locations representative of the range of possible engine locations above the wing. The sound field around the model was measured with an array of microphones on a rotating hoop that is also translated along an axis parallel to the airframe axis. The sound survey was repeated with the model wedge removed and the source in the nacelle only in place. The insertion loss was determined from the difference between the two resulting contours. Although no attempt was made to simulate the noise characteristics of a particular engine, the broadband noise source radiated sound over a range of scaled frequencies encompassing 1 and 2 times the blade passage frequency representative of a large, high-bypass-ratio turbofan engine. The data measured in this study show that significant shielding of the inlet-radiated noise is obtained in the area beneath and upstream of the model. The maximum insertion loss of the airframe is on the order of 20 dB at the relatively high blade passage frequency and is approximately 14 dB for the low-frequency-dominated broadband. The data show the sensitivity of scattering and diffraction to engine location, in particular the decreased insertion loss downstream of the airframe as the engine is moved aft. Although the complete analytical study is planned, a simplified insertion loss analysis was performed by using diffraction around a semi-infinite barrier. The measured and analytical results show comparable insertion loss under the wedge-shaped airframe at the scaled blade passage frequency.

Introduction

Increasing awareness of aircraft noise in areas surrounding airports has led to renewed emphasis on aircraft noise reduction at the source. In order to meet the aggressive noise impact reduction goals of the National Aeronautics and Space Administration (NASA) of the next 20 years, noise reduction must be an integral part of the airframe design process. The blended wing body (BWB) is an unconventional transport concept that has the potential to address long-term NASA goals for emissions, safety, capacity, cost of travel, and noise. The BWB combines a rigid, wide airframe shaped fuselage with high-aspect-ratio wings and semi-buried engines. A typical installation calls for three high-bypass-ratio engines, one over the centerbody and two outboard. The engines are mounted on top of the wing, aft of the passenger compartment. Inlet-radiated noise is shielded in the area below the aircraft by the wing upper surface.

A recently completed study on an early model of the BWB concept airframe verified significant shielding of the inlet-radiated noise by the fuselage (ref. 1). In addition to verifying inlet noise shielding, the data were to be used to validate an analytical program which is under development through NASA. The purpose of the program is to estimate the effect of installation on engine noise radiated from aircraft during flyover. Initial comparison of measured with estimated insertion loss was promising. Because the configuration of the BWB model used in the experiment is fixed, varying the parameters to any large extent is not possible. A follow-on program was undertaken to provide a broader database of noise shielding for the wedge-shaped airframe. The variation of parameters, in particular engine location, provides data with which to test the sensitivity of the analytical model. This report summarizes the experimental part of the follow-on project.

Experiment

Description of Model

Figure 1 shows a photograph of the model in the anechoic chamber of the Langley Anechoic Noise Research Facility (ANRF). The circular hoop in the

foreground is a microphone array that is discussed in the section "Facility and Experimental Setup." The wedge-shaped airframe is a triangular planform 36 in. (914.4 mm) long with a wingspan of 72 in. (1828.8 mm). It is 8 in. (203.2 mm) high at the center of gravity and tapers to approximately 1 in. (25.4 mm) thickness at the base. The model is made of pressed board for mass and is painted with acrylic paint to make the surface highly reflective. The model is supported on a sting that attaches to the base at the center of gravity. The sting is 48 in. (1219.2 mm) long and is wrapped with acoustic foam to minimize sound reflection, as is the mast which supports the sting. Although the model is intended only to be a representation of the blended wing body, its dimensions correspond approximately to 2 percent of the full-scale size. The engine nacelle is represented by a duct made of polyvinyl chloride (PVC) pipe with a 3-in. (76.2 mm) inside diameter and 9.75 in. (247.7 mm) long. The noise source is comprised of four impinging air jets. The nacelle is supported from the pipe which feeds the impinging jet noise source so that the noise source and nacelle can be moved to different locations with respect to the fuselage.

Figure 2 shows the point noise source without the nacelle. The noise source consists of four impinging air jets. The impinging jet arrangement is designed to provide a high frequency, high intensity broadband point noise source that is well suited to scale model work.

No effort was made to simulate either the frequency spectrum or the directionality characteristics of the high-bypass-ratio engines that are expected to be used in the BWB aircraft. Instead, the source used is omnidirective and broadband in order to radiate acoustic energy over the range of frequencies that the full-scale engine is expected to produce. For the inlet, tones may be expected to be generated at the blade passage frequency and its multiples. The blade passage frequency typical of a high-bypass-ratio engine is expected to be approximately 400 Hz, which corresponds to 20000 Hz in a 2-percent model. The combustion noise of the jet is expected to peak at a frequency on the order of 500 Hz, which would scale to 25000 Hz. Thus, the model noise source produces measurable acoustic energy at frequencies corresponding to the blade passage frequency tone and its first harmonic and to the peak in exhaust noise spectrum.

Facility and Experimental Setup

The experiment was conducted in the ANRF. The walls of the anechoic chamber are covered with fiberglass acoustic wedges that are 3 ft (0.915 m) deep and are designed to provide 99 percent absorption of incident sound above 100 Hz. The internal dimensions of the chamber (inside the tips of the acoustic wedges) are 28 by 27 by 24 ft (8.54 by 8.23 by 7.32 m). A more detailed description of the ANRF is given by Hubbard and Manning in reference 2. The mounting of the model on a sting allows for the microphone array to traverse around the model so that the sound field can be measured in three dimensions.

A microphone traverse system is a key part of the facility, and it allows for axial and azimuthal traverses. The circular hoop shown in figure 1 is mounted on a sled that can move in the axial direction on a linear track. The hoop contains 16 instrument-quality microphones which are equally spaced around the circumference. The microphones form a circle of 88 in. (2235.2 mm) in diameter. The hoop is rotated on 4° increments so that a high resolution map of the sound field is obtained in the azimuth. The entire hoop array is positioned at 15 axial locations, spanning from 12 in. (304.8 mm) upstream of the leading edge of the model to 7 in. (177.8 mm) downstream of the trailing edge. The specific linear track locations are chosen such that the microphone directly beneath the model moves in increments of 4° with respect to the sound source in the base position. Figure 3 shows the experiment layout including the model and the microphone array.

Instrumentation and Data Analysis

The acoustic sensors mounted on the hoop array are Brüel & Kjaer 1/4-in-diameter (6.4 mm) microphones. Noise measurements are acquired on a NEFF model 495 multichannel data acquisition system. The data acquisition system includes Precision filters set with a passband of 1000 to 50000 Hz. Data are collected in samples of 4-sec duration at a rate of 100000 samples/sec. The data acquisition system is driven by a DEC Alpha computer, which is also used to save the data and for postprocessing. All time histories are archived on optical disk and magnetic data tape.

2

All instrumentation components are calibrated on a regular schedule in accordance with ISO standards. In addition, an end-to-end calibration check of the data acquisition system is performed at the beginning and end of the test series by using a calibrated electromagnetic sound source. Samples of the time histories of each of the microphone responses are saved to files and the calibrated signals are used to check the sensitivities of the measurement microphones.

Description of Experiment

The impinging-jet source is placed in the center of the nacelle and acoustic surveys are taken around the model with the nacelle in six locations, three lateral and two axial for each lateral location, as summarized in table 1. The purpose of the lateral displacements is to investigate the shielding effect on side engines in a multiengine configuration. The axial locations include fore and aft. In the fore location, the leading edge of the nacelle is at the axial location of the model center of gravity. In the aft location, the trailing edge of the nacelle is as far downstream of the fuselage trailing edge as it was upstream of the trailing edge in the fore position. Fore and aft locations are used to show the loss of engine exhaust shielding when the nacelle discharge is downstream of the wing trailing edge. The base configuration is the one in which the nacelle is in the fore position with no lateral offset. The nacelle is always positioned 1/4 in. (6.4 mm) above the closest point on the model. Thus, when it is in the base position, the nacelle is 1/4 in. (6.4 mm) above the peak of the fuselage. As the source is moved laterally, it follows the slope of the line from the peak to the base of the fuselage. The nacelle retains the same height when it is moved from fore to aft.

The model fuselage is then removed and acoustic surveys made with the nacelle in the same locations. In this way, the insertion loss of the model wing can be calculated directly for each of the nacelle locations.

Table 1. Nacelle Locations Both With and Without the Model Present

[S is span from centerline to wingtip]

Nacelle axial location	Nacelle lateral offset		
Fore	0	S/4	S/2
Aft	0	S/4	S/2

Additional sound surveys are performed with the impinging-jet noise source in the nacelle positioned on the axis of the center of the hoop, with the nacelle removed and the source positioned on the axis of the center of the hoop and oriented parallel to the traverse axis, and with the source alone oriented perpendicular to the traverse axis. These surveys are intended to measure the directivity of the source alone and of the source in the nacelle.

Results

Narrowband fast Fourier transforms (FFTs) are performed on the acoustic data and are presented in this paper at the scaled blade passage frequency (20 000 Hz in the model scale). The broadband (1 to 25 kHz in the model scale) overall sound pressure level (OASPL) is also evaluated. The OASPL corresponds to the broadband noise of the spectrum without the influence of tones and generally accentuates the influence of low frequency noise sources. The data are presented as contour plots that give the noise as a function of azimuthal angle and axial location. The limited amount of data presented in this report is intended to show typical results for the experiment.

Noise Source

A representative spectrum of the noise emitted by the impinging-jet source is shown as the upper curve in figure 4. The source is relatively broadband from frequencies below 6 to 40 kHz. The lower curve in figure 4 is the background ambient sound level in the anechoic chamber. At frequencies above 10 kHz, the impinging-jet source produces noise that is at least 10 dB above the background ambient. Figure 5 shows a map of the directivity of the OASPL of the point source measured in the anechoic chamber. This map is a cylinder of sound around the source that has been unwrapped to show in two dimensions. The directivity plot shows a four-lobe pattern that comes from the four jets. The scale has been exaggerated to show the details of this lobe pattern, and the figure shows that the variation in sound level at any azimuth is no more than 2.0 dB.

Noise Measurements Without Model Present

Figure 6 shows a contour plot of the measured noise in the 20-kHz narrowband from the point source

3

in the nacelle in the base position without the wing present. The outline in the figure shows the location of the nacelle. The abscissa is the axial distance in inches. The ordinate is the azimuthal directivity angle in degrees, where 0° is below the model and 180° is above the model. The source in the base position is at a height of 84 3/4 in. (2152.7 mm), where the center of the hoop array is at 72 in. (1828.8 mm). Thus, the microphones above the model are closer to the source than the microphones below the model; this explains why the sound level appears to be higher above the nacelle than below it in figure 6. Moving the source aft as shown in figure 7 or laterally as shown in figure 8 shifts the contour in an equivalent way.

Noise Measurements With Model Present

Figure 9 shows a contour plot of the 20-kHz narrowband noise from the point source in the nacelle in the base position with the wing present. The outline of the wing is superimposed on the contour and shows the arc above the model (90° to 270° azimuth) and below the model (0° to 90° and 270° to 360° azimuth). The inlet-radiated noise is scattered up and slightly to the sides because of the slope of the wing from the peak to the side edges. Similarly, the discharge-radiated noise is scattered up and to the sides because of the taper from the peak to the trailing edge. The source noise is scattered away from the region below the model, and the contours of equal sound level follow the approximate shape of the wing.

Moving the source to the aft position increases the sound radiation to the rear above the model, as seen in figure 10. This increase is not only because of the rearward translation of the source but also because some of the inlet-radiated noise is reflected from the taper on the backside of the model in addition to the discharge-radiated noise. The noise level directly beneath the wing and well upstream from the leading edge is slightly less than it is for the nacelle in the fore position. Because inlet-radiated noise is dominant in the region, moving the source back increases the effective barrier height between the source and receiver; thus, the shielding effect is increased. The noise level directly below the model and toward the trailing edge is approximately 3 dB higher with the nacelle in the aft position than in the fore position. This indicates a significant noise shielding benefit by

positioning the nacelle discharge upstream of the trailing edge.

The effect of moving the source laterally (to simulate the effect of an outboard engine) is shown in figure 11. Inlet-radiated noise is scattered above the model predominantly toward the side of the model on which the source is located, and the area in which noise is reduced under the model is foreshortened. This configuration has the outboard nacelle location at halfway from the centerline of the fuselage to the wingtip. It is expected that no engine configuration would include an offset greater than one half the wing.

Noise Shielding by Airframe

Figure 12 is the measured insertion loss of the model airframe at 20 kHz for the source in the base position. The insertion loss is evaluated from the arithmetic difference of the narrowband noise level with the wing present and the noise level with the wing absent for the source in the base position. Negative decibel levels in the contour indicate noise reduction. The airframe scatters inlet- and discharge-radiated noise into the area above the model; thus, the sound level is increased. The noise is reduced below the model, more in the upstream direction than in the downstream. The maximum insertion loss is near the leading edge of the model at azimuthal angles offset from directly underneath by approximately 20°.

Moving the nacelle to the aft position increases the noise scattering in the downstream direction above the model, as shown in figure 13. Below the model, the insertion loss is nearly equal to 0; this indicates that none of the aft-radiated noise is shielded by the airframe. The area of maximum insertion loss under the model is shifted downstream by a distance equal to the downstream shift of the noise source.

Figure 14 shows the effect on insertion loss of moving the noise source laterally. Generally the contours of insertion loss shift in proportion to the source location. The area of maximum insertion loss under the airframe is foreshortened on the source side and elongated on the side opposite the source.

Figure 15 shows the overall insertion loss of the airframe with the source in the base position. This broadband insertion loss includes low frequency noise

4

emission, for which the shielding is expected to be less because of diffraction of noise around the barrier. The broadband noise is scattered above the model and to the sides in a manner similar to that for the single frequency. Likewise, the maximum insertion loss is in an area under the wing, near the leading edge, and slightly offset from directly underneath. This is consistent with the findings for the single frequency. Although the patterns are similar, the magnitude of noise reduction is approximately 5 dB less for the broadband noise than for the single frequency.

Comparison With Expected Shielding for Source in Base Position at 20 kHz

A complete analysis of the noise shielding by this airframe design is currently underway. A simplified analysis was performed by using theory for the diffraction of a semi-infinite barrier in the acoustic free field as shown in Irwin and Graf (ref. 3). The insertion loss (IL) is calculated from

$$IL = 10 \log(D) \qquad (1)$$

where

$$D = \sum_{i=1}^{N} \frac{\lambda}{3\lambda + 20\delta_i}$$

λ wavelength of sound, m

δ_i difference in length between direct path from source to receiver and path over barrier from source to receiver, m

N number of paths

In the relationship in equation (1), a negative number for insertion loss indicates noise reduction. The source is chosen to be at the nacelle inlet in the base position, and the frequency is 20 kHz. The insertion loss is evaluated for three paths: one over each of the sides of the wing and one over the trailing edge. Equation (1) does not estimate the noise increase due to scattering, and in fact the minimum estimated insertion loss is approximately −4.8 dB. The insertion loss is assumed to go to zero for any configuration in which there is a direct line of sight between the source and the receiver. The estimated insertion loss

under the wing at 20 kHz with the source in the base position is shown in figure 16. Results from this configuration compare with the measured results shown in figure 12. Although equation (1) cannot evaluate noise increase, for comparison purposes the same scale is used for figure 16 as for figure 12. The cutoff line at which insertion loss is zero is comparable between the measured and calculated results. The range of angles over which noise is reduced from the measurement extends from 288° to 68° at the leading edge of the model. The range is maximum at a point 5 in. (127.0 mm) upstream from the trailing edge, where the range is from 275° to 85°. The range of noise reduction from the calculated insertion loss is from 293° to 67° at the leading edge. The range is maximum at the trailing edge where it extends from 275° to 75°. The insertion loss increases from 0 to −17 dB as the observer moves deeper into the shadow zone at a rate that is comparable between the measured and the calculated results. The insertion loss is calculated to continue increasing to a maximum on the order of −20 dB directly under the wing, whereas the measured results show the insertion loss actually increases as the observer moves toward the locations beneath the model. The insertion loss contours wrap around the corner of the wing at the trailing edge for the calculated as well as the measured results, although the measured insertion loss values are considerably less than calculated in the area immediately downstream of the trailing edge in the measured data.

Concluding Remarks

A database has been generated in which the effect of source location on shielding effectiveness is assessed for a simplified wedge-shaped airframe. The scattering and diffraction of sound are found to be sensitive to the location of the source and to the shape of the airframe. The shielding is determined at the frequency of 20 kHz, which scales to the expected blade passage frequency of 400 Hz for a full-size aircraft. The maximum noise reduction is found to occur in the forward sector beneath the airframe. The tapered sides of the upper surface of the airframe scatter incident sound forward and above the model when the source is located in the forward position and toward the rear when the source is in the aft position. Moving the source laterally shifts the maximum shielding zone toward the side opposite beneath the wing. Although 20 kHz is a relatively high frequency in comparison to

the scale of the model, the broadband overall sound pressure level emphasizes lower frequencies. The broadband insertion loss contour is similar to the 20-kHz insertion loss contour except that the magnitude of insertion loss is less for broadband noise, and the noise reduction directly beneath the airframe is more evident.

The main purpose for this database is to validate an improved noise scattering analytical model that is currently being written by researchers at the Langley Research Center. While this comprehensive model is being completed, a simplified analysis using semi-infinite barrier diffraction is used to estimate the shielding by the triangular airframe shape. The measured and calculated insertion losses are comparable except in the areas directly under the wing and downstream of the trailing edge. The discrepancy between measured and calculated insertion losses directly under the airframe is believed to be due to the fact that

the sound level under the wing with the wing in place is near the background ambient so that the true insertion loss is limited by the noise floor in the anechoic chamber. This difference downstream is believed to be due to the contribution of the nacelle discharge radiated noise, which noise source is not included in the calculations.

References

1. Clark, Lorenzo R.; and Gerhold, Carl H.: Inlet Noise Reduction by Shielding for the Blended-Wing-Body Airplane. AIAA-99-1937, 1999.

2. Hubbard, Harvey H.; and Manning, James C.: *Aeroacoustic Research Facilities at NASA Langley Research Center.* NASA TM-84585, Mar. 1983.

3. Irwin, J. D.; and Graf, E. R.: *Industrial Noise and Vibration Control.* Prentice-Hall, Inc., 1979.
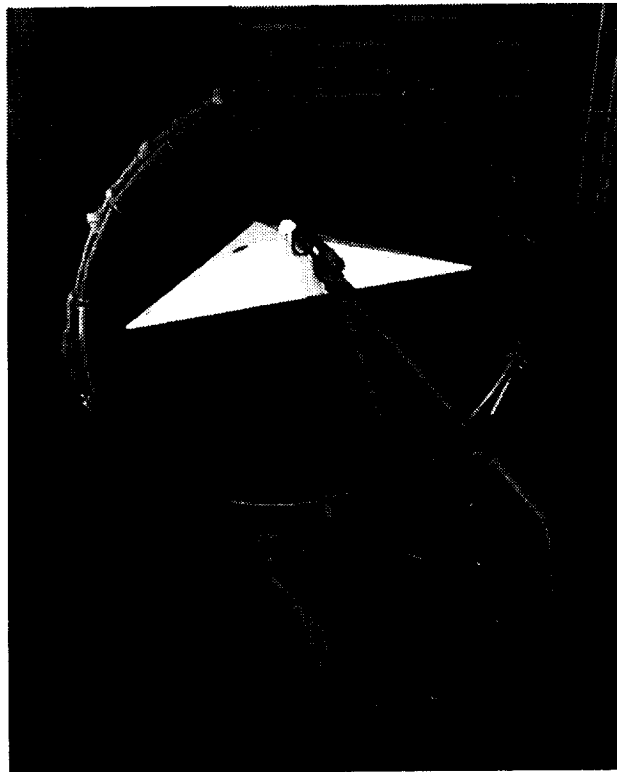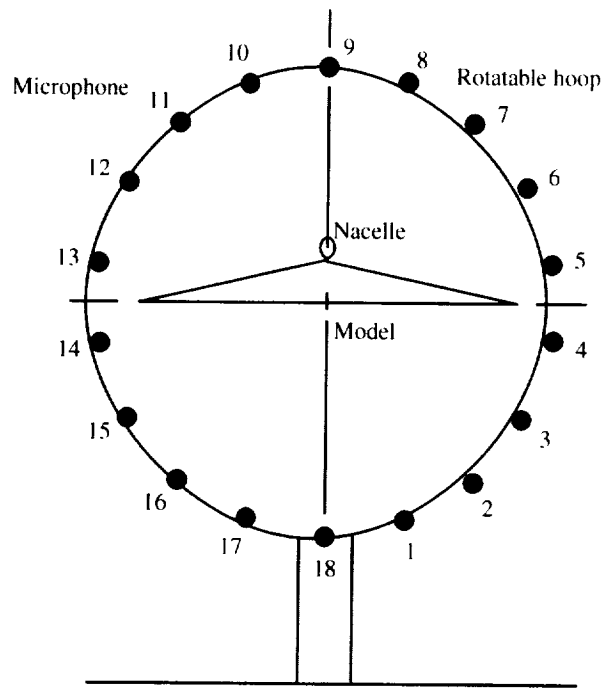
L-00-00538

Figure 1. Setup of wedge-shaped airframe model experiment in anechoic chamber. View looking upstream.
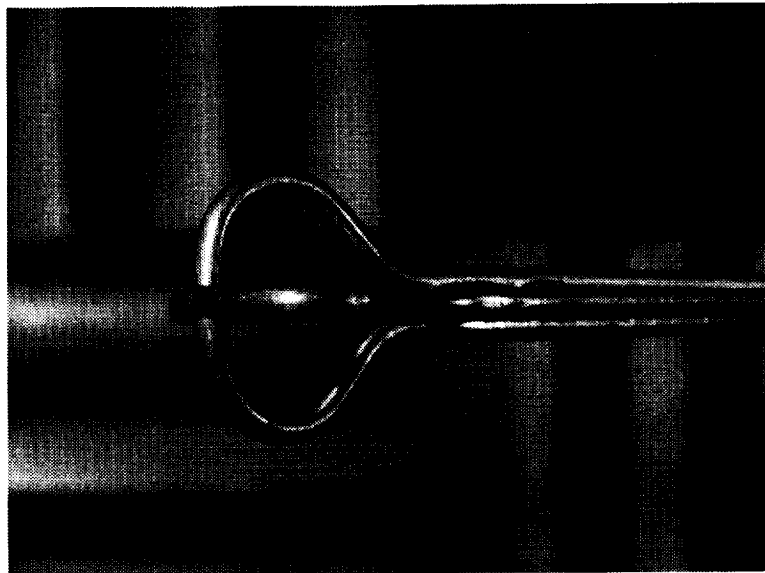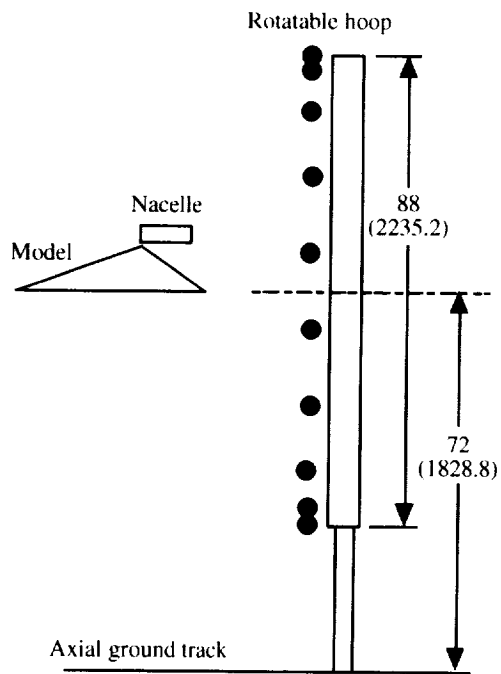

L-98-01585

Figure 2. Closeup of impinging-jet point noise source.

7

(a) End view.

(b) Side view.

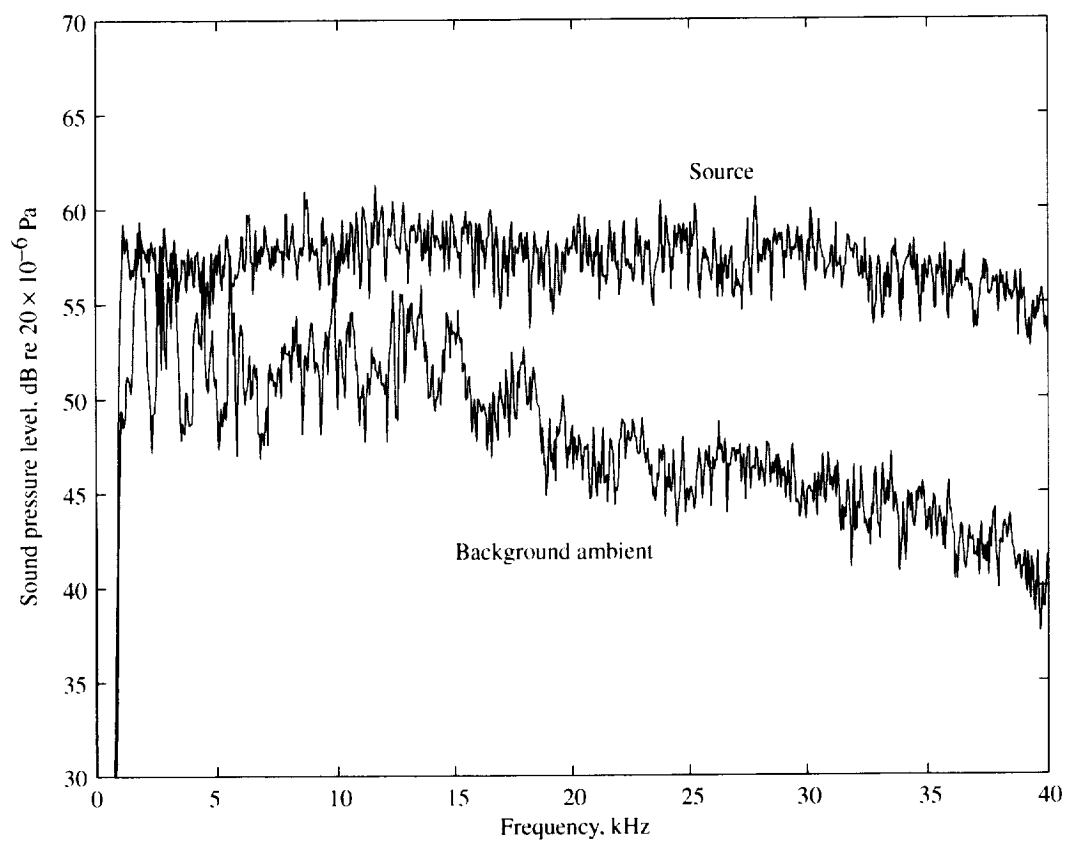Figure 3. Experiment setup. Dimensions are in inches (millimeters).

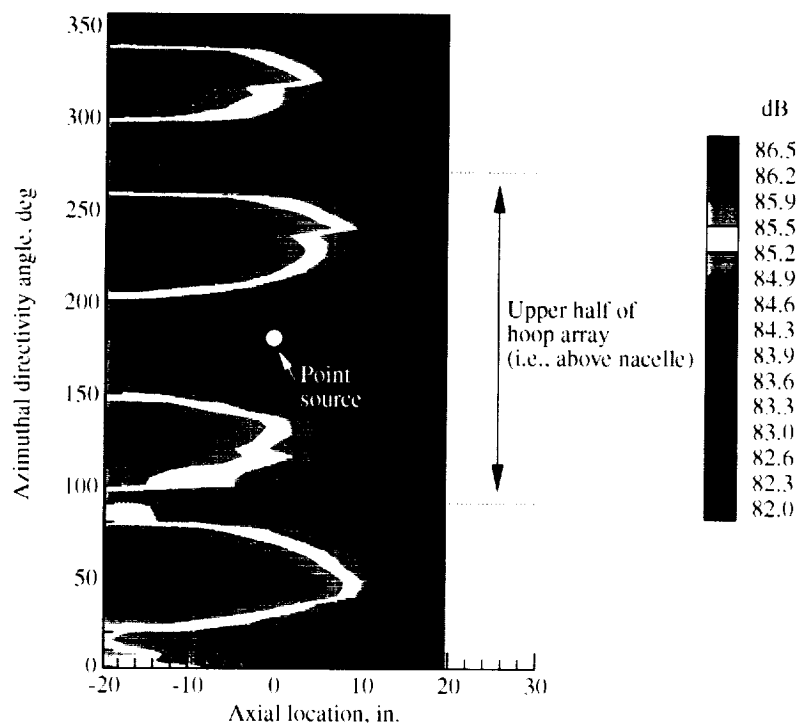Figure 4. Narrowband sound level spectrum for impinging-jet source.

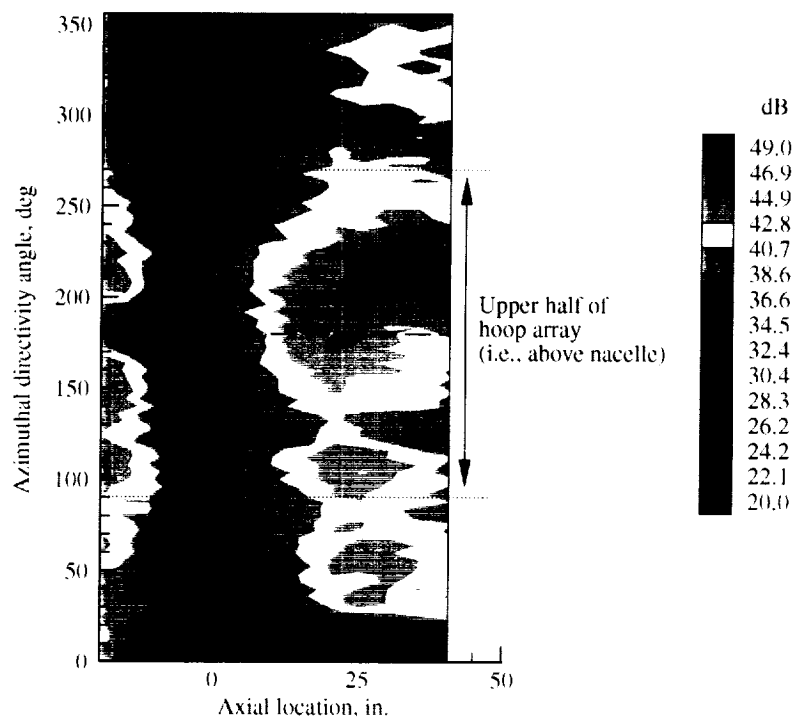Figure 5. OASPL directivity contour of impinging-jet point source.

Figure 6. Contour of noise radiation at 20 kHz, source in nacelle at base position, and without model wing.

10
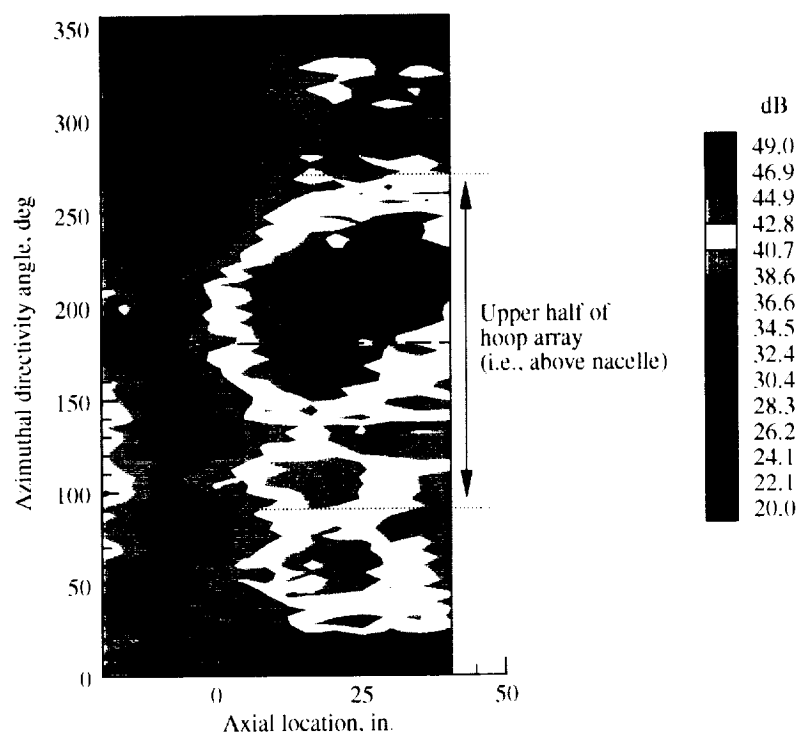
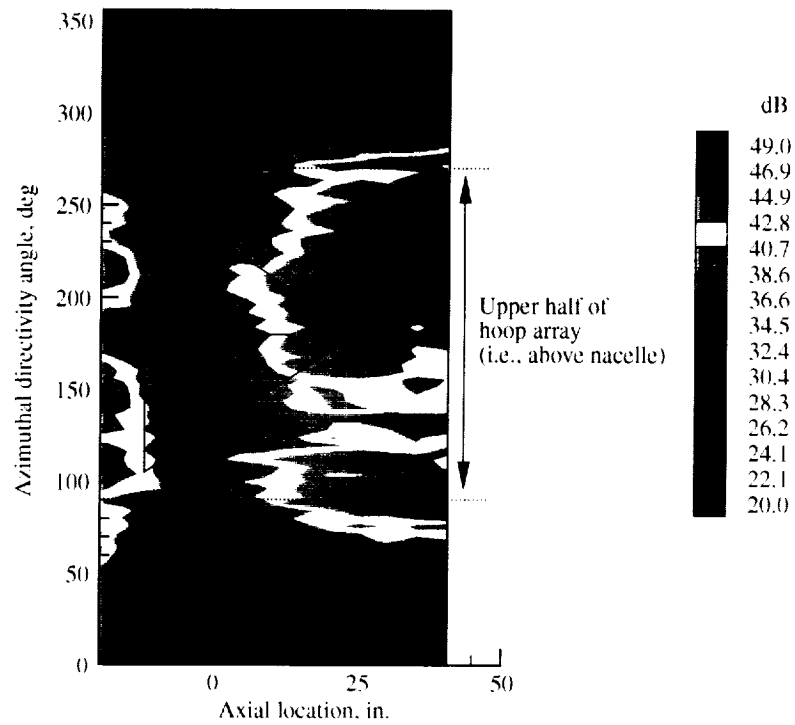Figure 7. Contour of noise radiation at 20 kHz, source in nacelle at 0 offset, aft location, and without model wing.
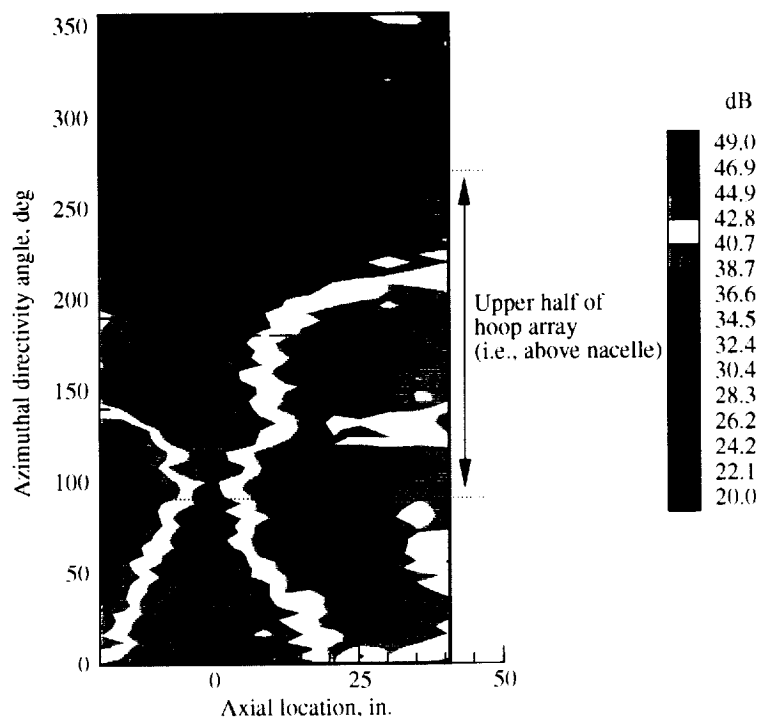
Figure 8. Contour of noise radiation at 20 kHz, source in nacelle at S/2 offset, fore location, and without model wing.

11

Figure 9. Contour of noise radiation at 20 kHz, source in nacelle at base position, and model wing present.
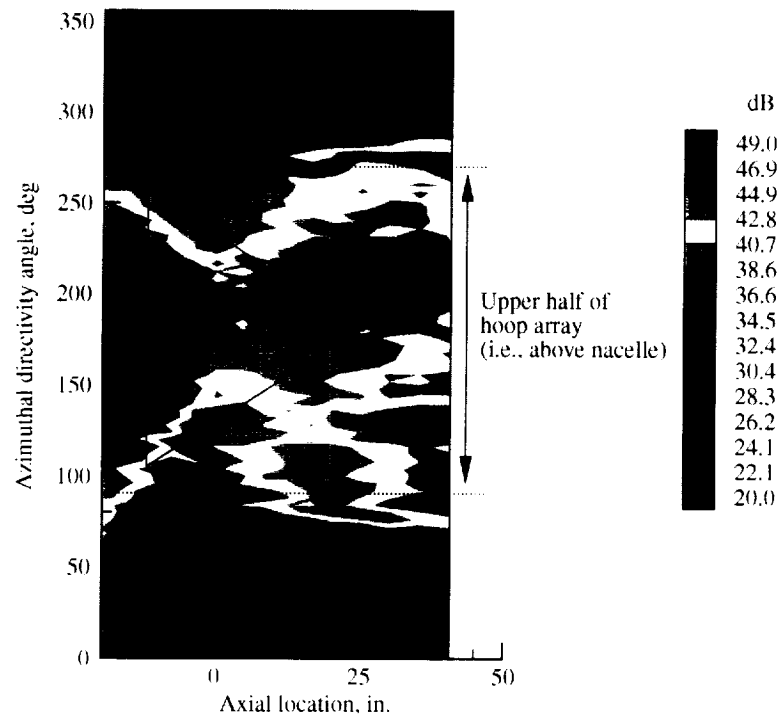

Figure 10. Contour of noise radiation at 20 kHz, source in nacelle at 0 offset, aft location, and model wing present.
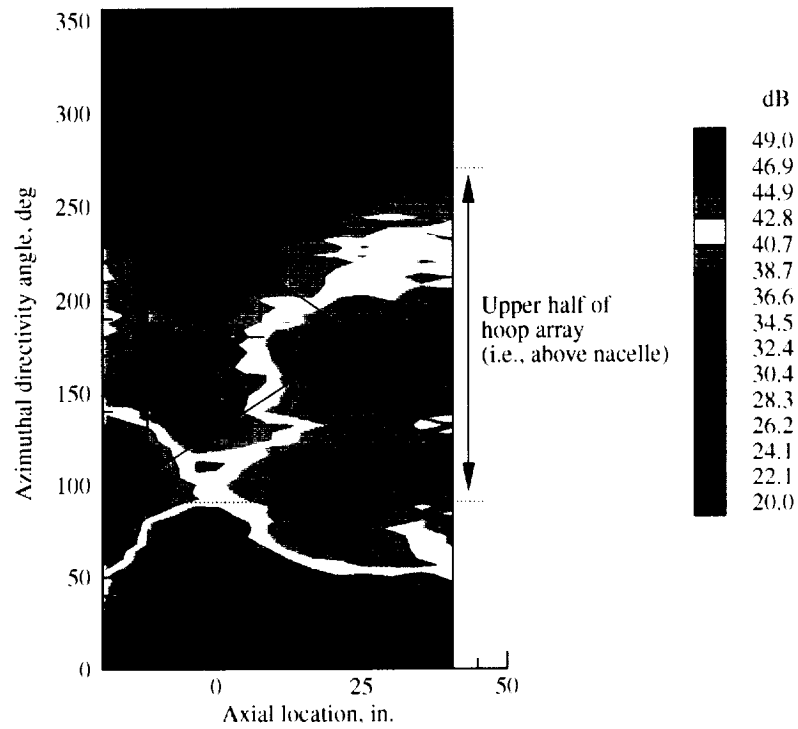
12

Figure 11. Contour of noise radiation at 20 kHz, source in nacelle at S/2 offset, fore location, and model wing present.
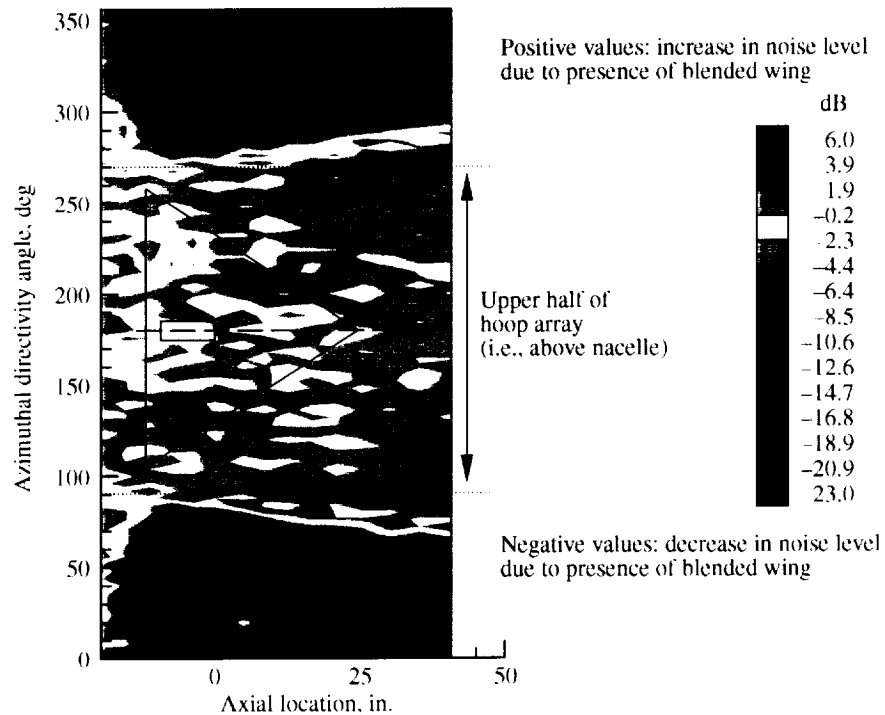

Figure 12. Contour of insertion loss at 20 kHz, source in nacelle at base position.
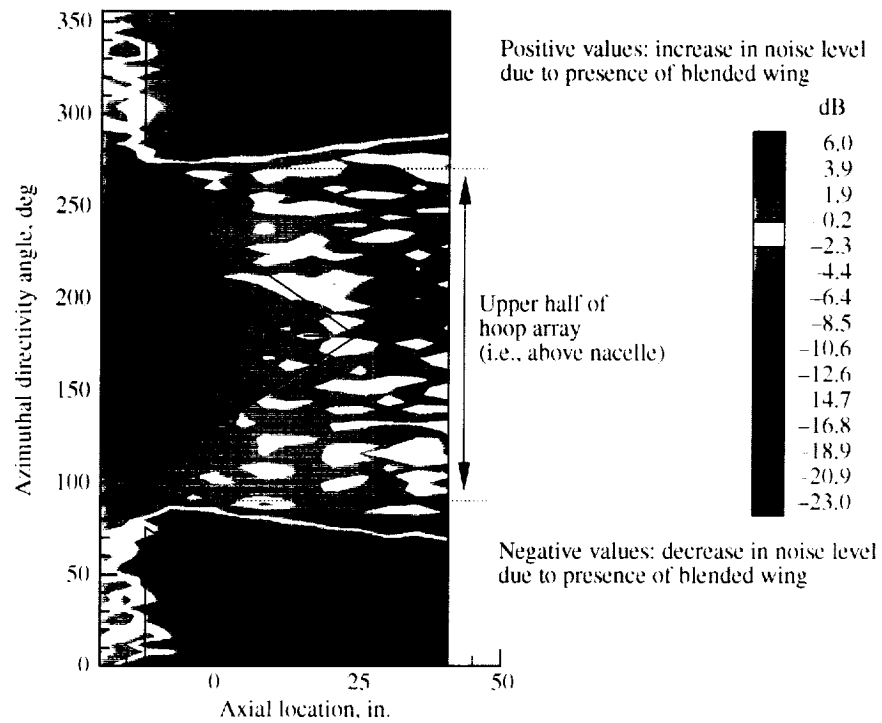
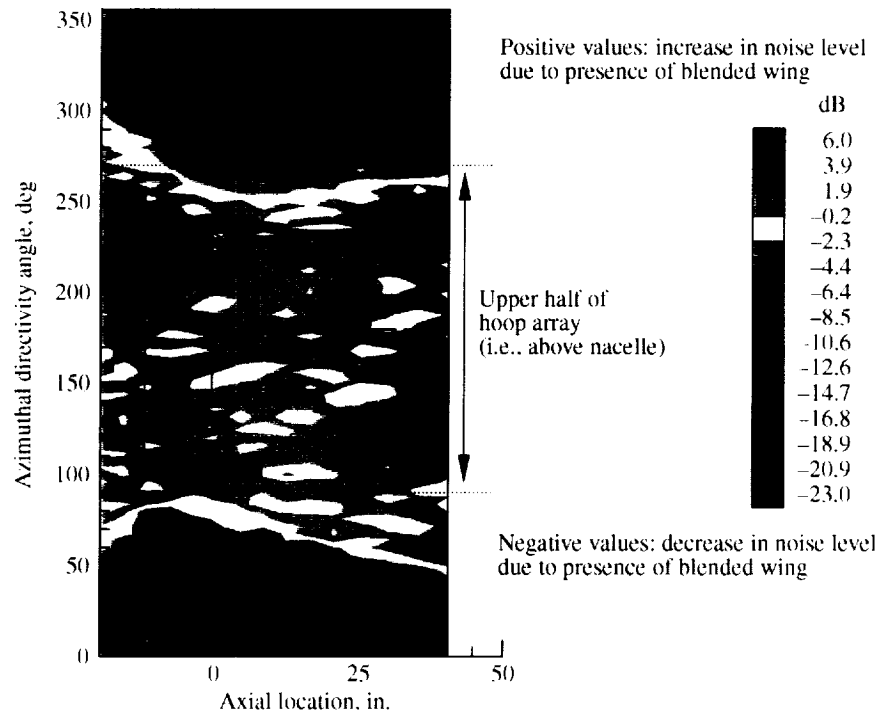Figure 13. Contour of insertion loss at 20 kHz, source in nacelle at 0 offset, and aft location.

Figure 14. Contour of insertion loss at 20 kHz, source in nacelle at S/2 offset, and fore location.
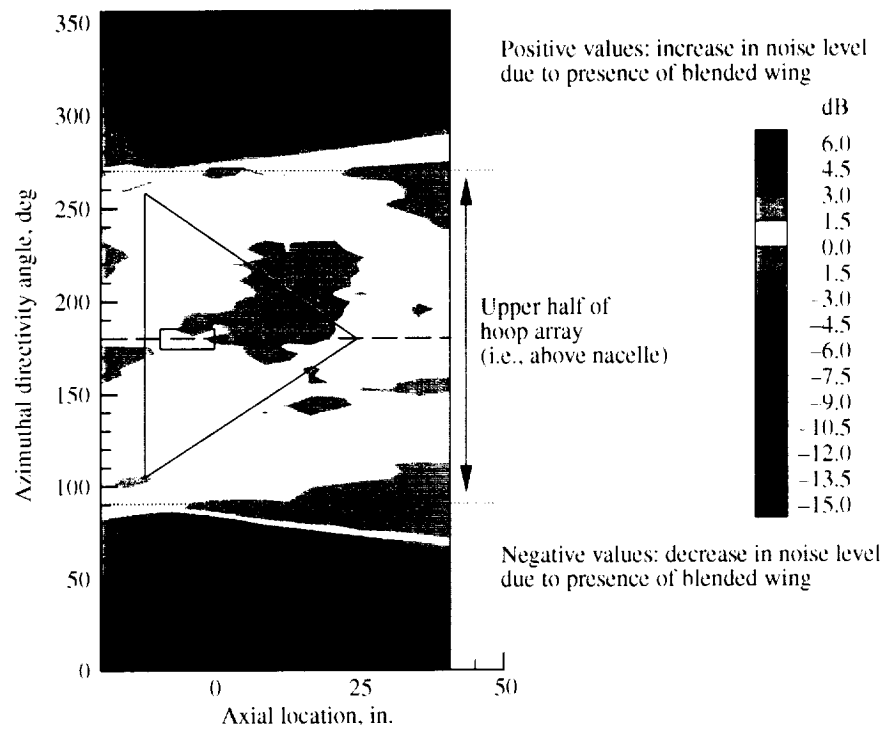
Figure 15. Contour of broadband noise insertion loss, source in nacelle at base position.
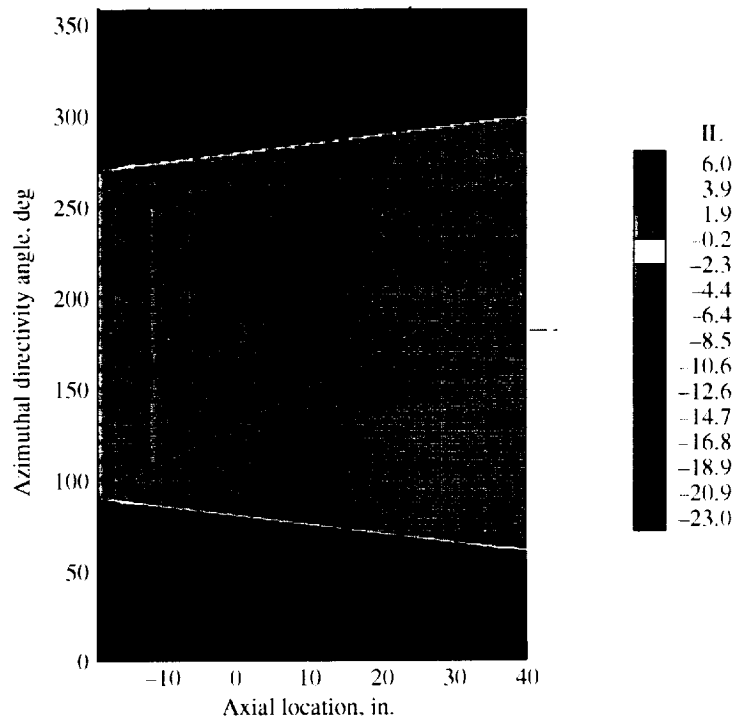

Figure 16. Calculated insertion loss of wedge-shaped airframe, source at inlet of duct, and 20 kHz frequency.

REPORT DOCUMENTATION PAGE

Public reporting burden for this collection of information is estimated to average 1 hour per response, including the time for reviewing instructions, searching existing data sources, gathering and maintaining the data needed, and completing and reviewing the collection of information. Send comments regarding this burden estimate or any other aspect of this collection of information, including suggestions for reducing this burden, to Washington Headquarters Services, Directorate for Information Operations and Reports, 1215 Jefferson Davis Highway, Suite 1204, Arlington, VA 22202-4302, and to the Office of Management and Budget, Paperwork Reduction Project (0704-0188), Washington, DC 20503.

1. AGENCY USE ONLY *(Leave blank)*	2. REPORT DATE April 2001	3. REPORT TYPE AND DATES COVERED Technical Memorandum	
4. TITLE AND SUBTITLE Database of Inlet and Exhaust Noise Shielding for Wedge-Shaped Airframe		**5. FUNDING NUMBERS** WU 706-81-12-01	
6. AUTHOR(S) Carl H. Gerhold and Lorenzo R. Clark			
7. PERFORMING ORGANIZATION NAME(S) AND ADDRESS(ES) NASA Langley Research Center Hampton, VA 23681-2199		**8. PERFORMING ORGANIZATION REPORT NUMBER** L-18053	
9. SPONSORING/MONITORING AGENCY NAME(S) AND ADDRESS(ES) National Aeronautics and Space Administration Washington, DC 20546-0001		**10. SPONSORING/MONITORING AGENCY REPORT NUMBER** NASA/TM-2001-210840	

11. SUPPLEMENTARY NOTES

12a. DISTRIBUTION/AVAILABILITY STATEMENT Unclassified–Unlimited Subject Category 71 Distribution: Standard Availability: NASA CASI (301) 621-0390	12b. DISTRIBUTION CODE

13. ABSTRACT *(Maximum 200 words)*

An experiment to measure the noise shielding of the blended wing body design concept was developed using a simplified wedge-shaped airframe. The experimental study was conducted in the Langley Anechoic Noise Research Facility. A wideband, omnidirective sound source in a simulated engine nacelle was held at locations representative of a range of engine locations above the wing. The sound field around the model was measured, with the airframe and source in place and with source alone, using an array of microphones on a rotating hoop that is also translated along an axis parallel to the airframe axis. The insertion loss was determined from the difference between the two resulting contours. Although no attempt was made to simulate the noise characteristics of a particular engine, the broadband noise source radiated sound over a range of scaled frequencies encompassing 1 and 2 times the blade passage frequency representative of a large, high-bypass-ratio turbofan engine. The measured data show that significant shielding of the inlet-radiated noise is obtained in the area beneath and upstream of the model. The data show the sensitivity of insertion loss to engine location.

14. SUBJECT TERMS Noise shielding; Blended wing body; Model scale; Source location			15. NUMBER OF PAGES 20
			16. PRICE CODE A03
17. SECURITY CLASSIFICATION OF REPORT Unclassified	18. SECURITY CLASSIFICATION OF THIS PAGE Unclassified	19. SECURITY CLASSIFICATION OF ABSTRACT Unclassified	20. LIMITATION OF ABSTRACT UL